Journal of Catalysis 263 (2009) iii–vii

Contents lists available at ScienceDirect

Journal of Catalysis

www.elsevier.com/locate/jcat

Journal of Catalysis Vol. 263, No. 2, 2009

Contents

REGULAR ARTICLES

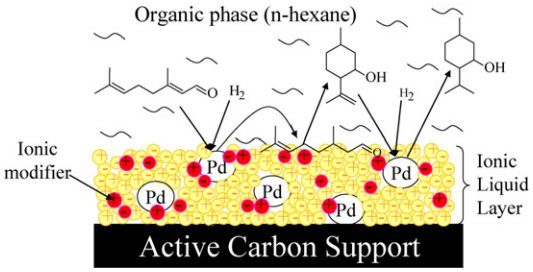

Supported Ionic Liquid Catalyst (SILCA) was modified with different Lewis and Brønsted acids and the effects of different acids to the catalyst activity and product selectivity in a reaction of menthols from citral was evaluated.

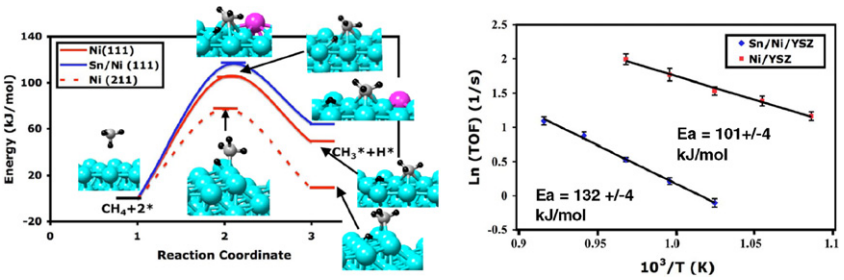

Sn atoms dispersed on supported Ni catalysts alter catalytic methane steam reforming by (i) changing the nature of the active sites, (ii) increasing the overall activation barrier, and (iii) improving the catalyst tolerance to carbon-induced deactivation.

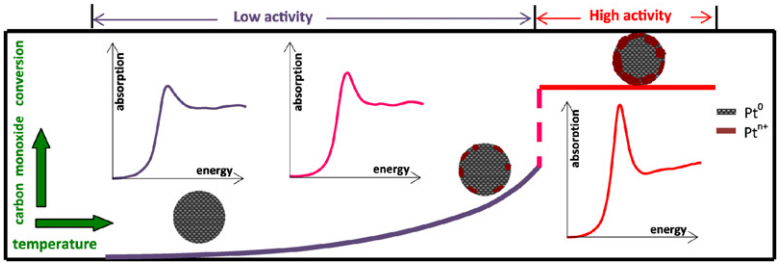

In situ XAS identified surface-oxidized platinum as the active species at high activity during carbon monoxide oxidation over supported platinum catalysts. At low activity, the platinum catalysts were metallic and poisoned by carbon monoxide.

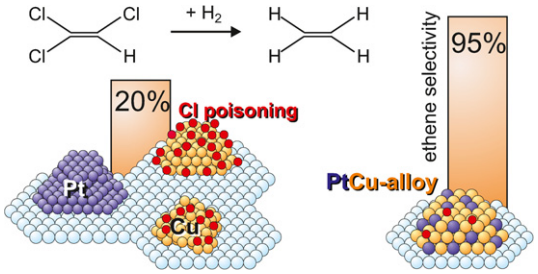

Pt (or Pd)–Cu alloy nanoparticles show superior performance in the selective hydrodechlorination of trichloroethene to ethene, as compared to catalysts containing separated particles of Pt (or Pd) and Cu. The reaction proceeds via cleavage of the C–Cl bond on Cu, with the Cu site being subsequently regenerated by spillover of hydrogen from the noble metal.

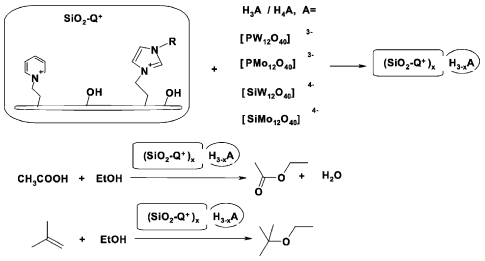

Oniumsilica-immobilized heteropolyacids display good catalytic performance and relative high structural stability in the liquid-phase synthesis of ETBE and the esterification of AcOH with EtOH.

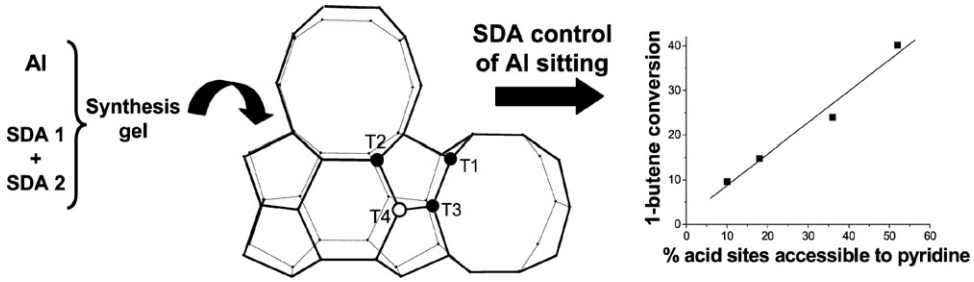

Al sitting in ferrierite crystals has been controlled by carrying out the zeolite synthesis with selected combinations of organic directing agents in fluoride medium. The catalytic activity for the isomerisation of linear butenes and *m*-xylene increased as the relative population of strong Brönsted acid groups in sterically constrained sites inside the ferrierite cavity decreased.

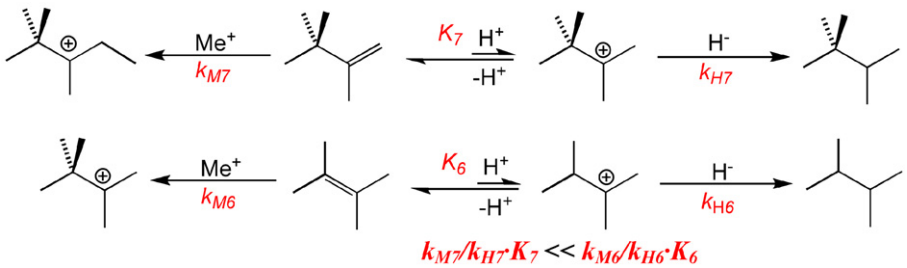

The relative rate of olefin homologation by cationic methylation vs. hydrogenation by protonation/hydride transfer increases with the degree of substitution of the olefin, a trend that explains the remarkably high selectivity observed for conversion of methanol to triptane over zinc and indium iodides.

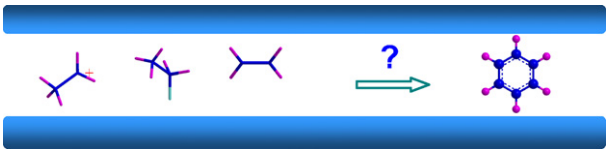

The acidity and pore size of zeolites strongly affect their catalytic behavior. *In situ* MAS NMR studies indicate that the transition state shape selectivity in the ethylbenzene disproportionation and the formation of alkylcarbenium ions are responsible for oligomerization and coke formation.

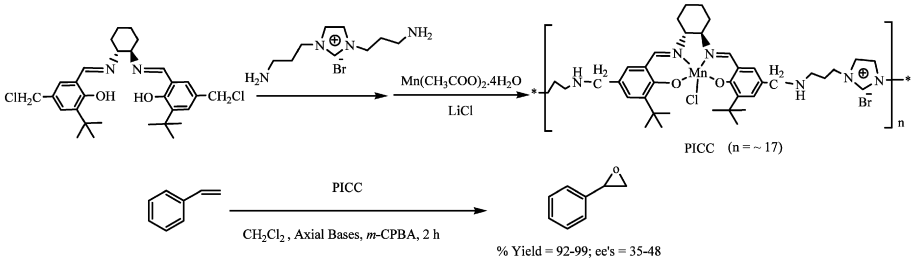

A novel polymeric ionic liquid-functionalized chiral salen Mn(III) complex was found to be an efficient catalyst for enantioselective epoxidation of styrene and can be recycled easily by control of solvent.

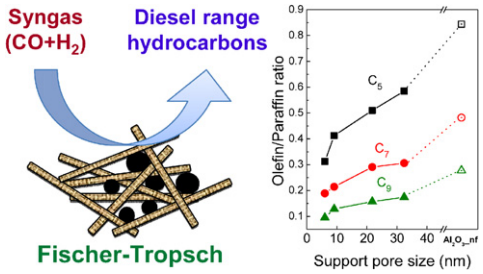

CoRu Fischer–Tropsch catalysts supported on macro-mesoporous nanofibrous γ-Al_2O_3 reconcile high metal dispersions with enhanced intrapellet transport rates resulting, at high metal loadings, in improved productivity to diesel-range hydrocarbons.

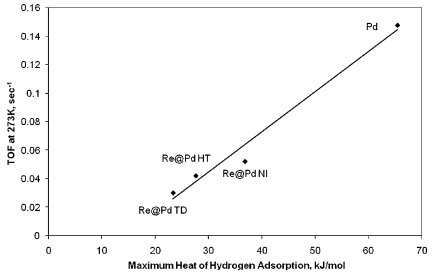

Bimetallic overlayer Pd on Re (Re@Pd) catalysts showed decreased H_2 heat of adsorption and ethylene hydrogenation activity compared to Pd. A correlation relating hydrogen adsorption strength and activity was developed.

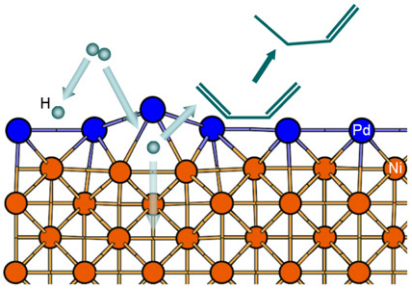

Palladium surfaces become more active hydrogenation catalysts if hydrogen dissolution into the metal can be blocked.

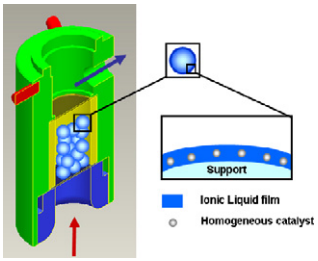

Supported Ionic Liquid Phase (SILP) catalytic materials have been employed in the gas-phase hydroformylation of 1-butene. In order to study the intrinsic kinetics of the immobilized rhodium-diphosphine catalyst complex, a gradient-free loop reactor (Berty-type) has been employed. Data from fixed bed and Berty reactor were found to be in good agreement with respect to activation energy and reaction order. Ex-situ NMR studies of fresh and used SILP catalysts confirmed that the ligand remained intact after prolonged time on stream.

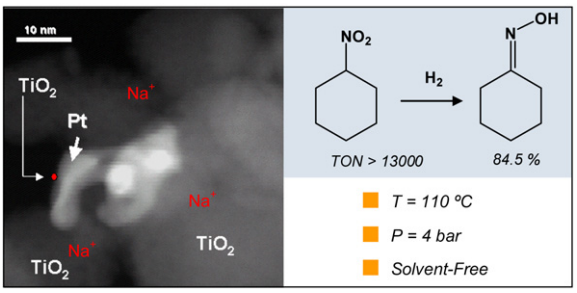

Acid-free decorated Pt/TiO_2 catalyst promotes the selective hydrogenation of nitrocyclohexane to cyclohexanone oxime under green and mild reaction conditions.

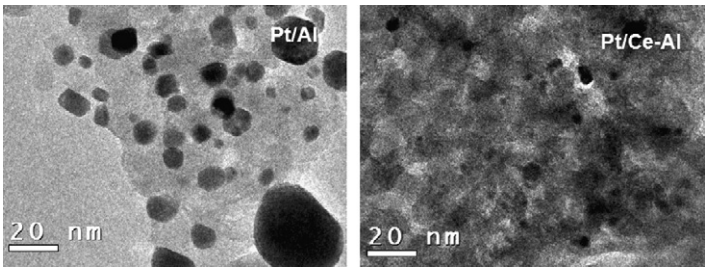

Addition of Ce to Pt/Al_2O_3 catalysts increases their performance in methane reforming, due to the improved thermal stability of the support and the interaction of reduced Pt nanoparticles with Ce, which prevents their migration.

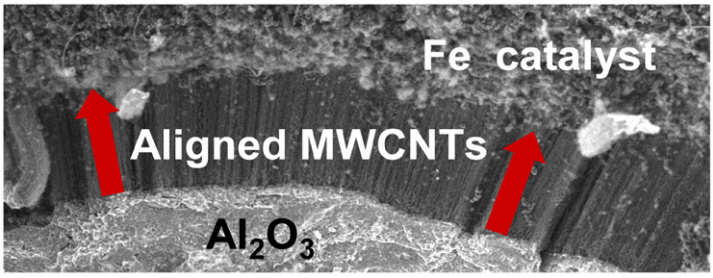

MWCNTs grow aligned between the Al_2O_3 support and the iron surface catalytic film.

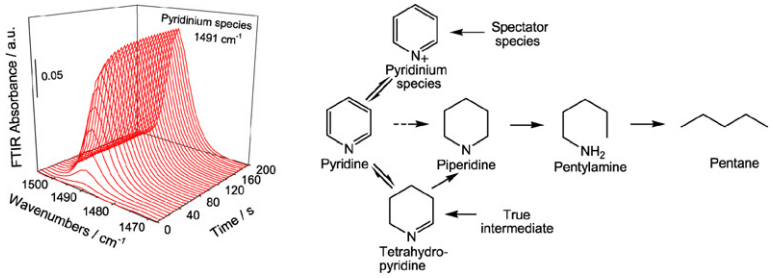

The transient reaction rate of a pyridinium species did not correspond to the overall reaction rate, demonstrating that mere observation of an adsorbed species is not sufficient to prove it is a reaction intermediate.

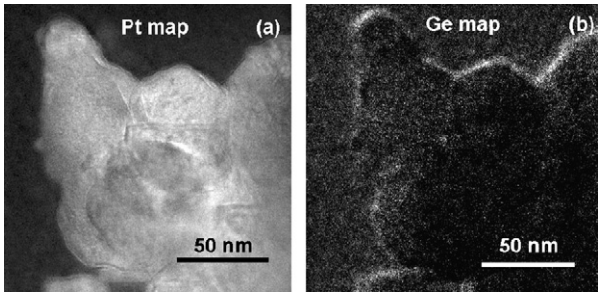

Ge deposited on to Pt black and Pt/SiO_2 occupied a fraction of edge sites on the surface (as shown on the EFTEM picture) and promoted the formation of saturated ring opening products from methylcyclopentane.

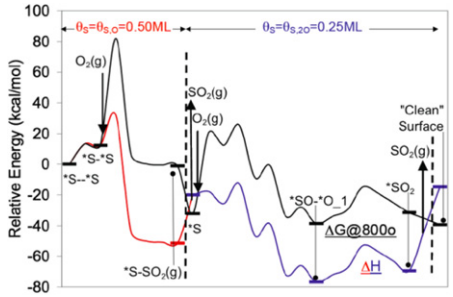

DFT calculations have revealed that the complete removal of sulfur adatoms from the sulfur-poisoned Ni(111) surfaces of the Ni-based SOFC anodes can be accomplished by direct oxidation during the post-treatment process.